

# Probabilistic Model for Mechanical Power Fluctuations in Asynchronous Wind Parks

José Cidrás Pidre, *Member, IEEE*, Camilo José Carrillo, and Andrés Elías Feijóo Lorenzo

**Abstract**—Wind parks and their impact on electrical power systems have become an important area for analysis over the last decade. Particularly, the influence of wind turbines on power quality of electrical power systems is today a subject of study for several electrical and wind turbine manufacturing companies, standards committees, and universities.

In this paper, a new probabilistic model for analyzing electrical power fluctuations from wind parks with asynchronous generators is developed. The model is based on the aggregation of the linearized electrical and mechanical equations for wind turbines, and it can be used for power quality analysis. The proposed model is also used for assessing voltage and current fluctuations and flicker emission in the wind park.

**Index Terms**—Asynchronous wind turbine, slow voltage fluctuation, synchronization of induction machines, wind energy, wind park.

## I. INTRODUCTION

WIND parks can affect an electrical power system in several ways: in its steady-state and dynamic security levels and in power quality. Steady-state security is concerned with wind power injected and line capacities of the electrical power system. For this analysis, probabilistic models of average wind speed and a load flow program are necessary [1]. For dynamic studies, dynamic models are needed. Power quality is related to high frequency fluctuations in wind power (units of Hertz) [2], [3], and, consequently, more complete wind models and dynamic simulations are used.

In general, several phenomena at different frequencies can be observed in the wind [4]. Yearly, monthly, and daily frequencies have traditionally been described in the spectrum of wind speed. This information is handled by probabilistic models [4], [5]. Other phenomena are known to be present in wind speed, such as turbulence, generally considered as normally distributed [6]. Turbulence can be responsible for an important amount of flicker emissions in a wind park.

The mechanical power of wind turbines has a similar spectrum to the wind speed. However, other mechanical power fluctuations take place in wind turbines. These fluctuations depend on the blade position and they are known as tower shadow

Manuscript received October 7, 2002. This work was supported in part by the Ministerio de Educación y Cultura under Contract PB98-1096-C02-01 and in part by Xunta de Galicia under Contract PGIDT00PXI32102PN.

J. C. Pidre is with the Departamento de Enxeñaría Eléctrica of the Universidade de Vigo, Campus de Lagoas, Vigo, Spain (e-mail: jcidras@uvigo.es).

C. J. Carrillo is with the Departamento de Enxeñaría Eléctrica of the Universidade de Vigo (e-mail: carrillo@uvigo.es).

A. E. F. Lorenzo is with the Departamento de Enxeñaría Eléctrica of the Universidade de Vigo (e-mail: afeijoo@uvigo.es).

Digital Object Identifier 10.1109/TPWRS.2003.811201

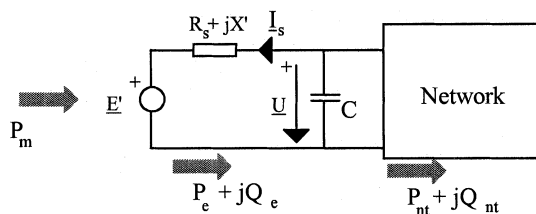


Fig. 1. Scheme of an asynchronous generator in front of the network.

and wind shear phenomena [3]. Several authors assume, based on measurements, that mechanical power fluctuations due to wind turbine rotational phenomena, can be simulated by a periodic (quasisinusoidal) function with the frequency of the blades passing in front of the tower (1–2 Hz) and a magnitude of approximately 10–20% of the average value [3], [7]. As these mechanical power fluctuations influence the modulus of voltage variations, power quality problems can be caused (flicker phenomenon).

This paper deals with modeling mechanical power fluctuations caused by wind turbine rotation in an asynchronous wind park. It is not the purpose of the paper to deal with the impact caused by turbulence, although it can affect power quality as mentioned before.

A single model for the complete wind park is used. To obtain this model it is necessary to aggregate the asynchronous generators in the wind park. Some authors obtain the aggregated model from the induction machine parameters [8], [9], [11], [12]. In this paper, the linear dynamic equations have been used for the same purpose [10].

The original aggregated model is used to define a probabilistic model, which is realistic, practical and easy. The model is used for assessing the fluctuations of electrical and mechanical variables, and flicker [2].

## II. DYNAMIC MODEL OF AN INDUCTION WIND GENERATOR

The induction generator can be modeled as a Thevenin equivalent voltage source  $\underline{E}'$  behind the impedance  $R + jX'$ , as can be seen in Fig. 1[13]. This dynamic model is defined by considering balanced work and neglecting the electromagnetic dynamic effects of the stator, and it is known as the third order induction machine model.

The parameters of the machine and definition of variables can be seen in Appendix II.

The value of  $\underline{E}'$  can be calculated by integrating the following equation:

$$\frac{d\underline{E}'}{dt} = -j\omega_s s \underline{E}' - \frac{1}{T_0} (\underline{E}' - j(X_0 - X') \underline{I}_s). \quad (1)$$

The electrical equation of the stator current is

$$\underline{I}_s = \frac{\underline{U} - \underline{E}'}{R_s + jX'} \quad (2)$$

The electromechanical equation can be written as

$$P_m - P_e = 2H(1-s) \frac{ds}{dt} \quad (3)$$

where

- $P_m$  is the mechanical power ( $P_m < 0$  for generation);
- $H$  is the inertia constant;
- $P_e$  is the real power.

The model of mechanical power can be expressed by the following terms:

$$P_m(t) = P_{m,0} + \Delta P_m \quad (4)$$

where

- $P_{m,0}$  represents the wind power with low frequencies, and it is obtained from the mean value of the wind, defined by a Weibull or a Rayleigh distribution [1], [14]. In this paper the  $P_{m,0}$  component of mechanical power is assumed to be constant;
- $\Delta P_m$  is the power fluctuation caused by tower shadow and wind shear effects, and rotational sampling, with a frequency of about 1-2 Hz.

Some measurements [7] taken in the stator of a wind turbine, together with the results presented by other authors [22], show that the main frequency related to power oscillation is that called 3P, which is three times the rotational speed and it is caused by tower shadow. Other frequencies can appear in the spectrum, specially the 1P component related to rotor unbalance [21], [23]. Nevertheless, the impact of the 3P component on flicker is higher than that of the 1P component due to its frequency range [24]. According to this, mechanical power fluctuations can be expressed as

$$\Delta P_m = P_s \sin \theta(t) \quad (5)$$

where

- $\Delta P_s$  is the amplitude of mechanical sinusoidal fluctuations;
- $\theta(t)$  is the mechanical angle of the turbine and is defined as

$$\theta(t) = \theta_0 + \int_{t_0}^t (1 - s_0 + \Delta s) \Omega_s dt \quad (6)$$

where

- $\theta_0$  is the initial mechanical angle;
- $s_0$  is the initial slip of the induction generator;
- $\Omega_s = 3 \cdot 2 \cdot \omega_s / (r \cdot p)$  is the synchronous speed of tower shadow effect in rad/s, where the synchronous speed of the turbine is  $2 \cdot \omega_s / (r \cdot p)$ ;
- $\omega_s$  is the synchronous speed of the induction generator ( $2 \cdot \pi \cdot 50$  in Europe) in rad/s;
- $r$  is the gear box ratio;
- $p$  is the number of poles.

The electrical power,  $P_e$ , is calculated as

$$P_e = P_e'(1-s) = \text{Re} \{ \underline{E}' \underline{I}_s^* \} \quad (7)$$

### III. LINEAR DYNAMIC MODEL OF AN INDUCTION GENERATOR

The linear dynamic model is based on the following considerations: i) The induction generator has an initial steady-state situation -operating point- defined by  $(\underline{E}'_0, s_0, \underline{I}_{s,0}, P_{m,0}, \underline{U}_0, \underline{V}_0)$ , and ii) The small changes in (1), (3), (6) and (7) are  $\Delta \underline{E}' / \Delta s \approx 0$ ,  $\Delta s \ll s_0$ ,  $\Delta \underline{E}' / \Delta \underline{E}'^* \approx 0$ ,  $\Delta \underline{E}' / \Delta \underline{U}^* \approx 0$  and  $\sin \Delta \theta = \Delta \theta \approx 0$ .

So, the linear dynamic model, taking into account (1)–(3), (5)–(7), can be calculated by integrating the following equations:

$$\frac{d\Delta \underline{E}'}{dt} = -z\Delta \underline{E}' - j\omega_s \Delta s \underline{E}'_0 + z' \Delta \underline{U} \quad (8)$$

$$\Delta P_m - \Delta P_e = h \frac{d\Delta s}{dt} \quad (9)$$

$$\Delta P_m(t) = P_s \sin(\theta_0 + \Omega_0 t) \quad (10)$$

$$\Delta P_e = \text{Re} \{ -y\Delta \underline{E}'^* + \underline{I}_{s,0}^* \Delta \underline{E}' + y\Delta \underline{U}^* \} \quad (11)$$

where

- $z = v + jw = j\omega_s s_0 + 1/T'_0 (1 + j(X_0 - X'/R_s + jX'))$
- $z' = v' + jw' = 1/T'_0 (X_0 - X'/R_s + jX')$
- $h = 2H(1-s_0)$
- $y = g + jm = \underline{E}'_0^* / (R_s - jX')$
- $\Omega_0 = (1-s_0)\Omega_s$

In matrix notation (8)–(11) can be expressed by a linear differential first order system

$$\frac{d}{dt} \begin{bmatrix} \Delta E^r \\ \Delta E^m \\ \Delta s \end{bmatrix} = \begin{bmatrix} -v & w & \omega_s E_0^m \\ -w & -v & -\omega_s E_0^r \\ -\frac{e}{h} & -\frac{f}{h} & 0 \end{bmatrix} \begin{bmatrix} \Delta E^r \\ \Delta E^m \\ \Delta s \end{bmatrix} + \begin{bmatrix} v' & -w' \\ w' & v' \\ -\frac{g}{h} & -\frac{m}{h} \end{bmatrix} \begin{bmatrix} \Delta U^r \\ \Delta U^m \end{bmatrix} + \begin{bmatrix} 0 \\ 0 \\ \frac{\Delta P_m}{h} \end{bmatrix} \quad (12)$$

where

- $\underline{E}' = E^r + jE^m$ ;
- $\underline{U}' = U^r + jU^m$ ;
- $e = I_{s,0}^r - g$ ;
- $f = I_{s,0}^m - m$ .

And (12) in condensed form

$$\frac{d\mathbf{x}}{dt} = \mathbf{A}\mathbf{x} + \mathbf{B}\mathbf{u} + \mathbf{b}\Delta P_m \quad (13)$$

where

- $\mathbf{A}$ ,  $\mathbf{B}$  and  $\mathbf{b}$  are, respectively, constant real matrices and a vector that are defined using parameters and initial values for wind turbines;
- $\mathbf{x}$  is the vector of unknown variables;
- $\mathbf{u}$  is the vector of voltage in the bus generators, and its value is related to the network;
- $\Delta P_m$  is the input variable (excitation source) and it represents the mechanical fluctuations of wind power.

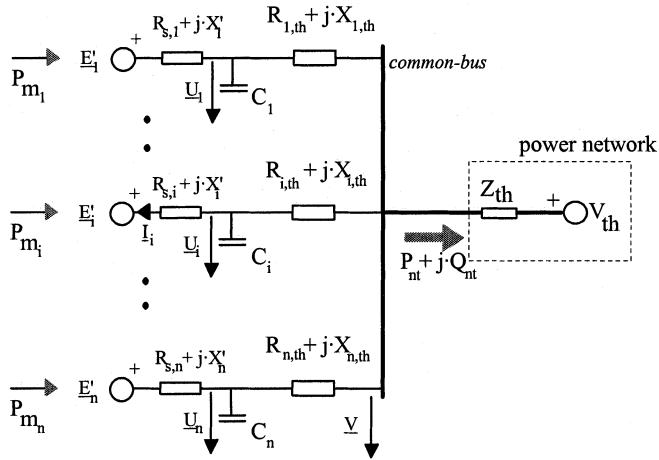


Fig. 2. Scheme of a wind park.

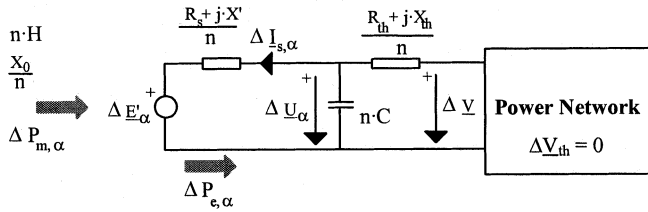


Fig. 3. Equivalent linear scheme of wind park.

#### IV. AGGREGATED LINEAR DYNAMIC MODEL OF A WIND PARK

Applying the linear dynamic model (13) to a wind park with  $n$  wind turbines (Fig. 2), the following equations can be written:

$$\left[ \frac{dx_i}{dt} \right] = [A_{i,i}x_i] + [B_{i,i}u_i] + [b_i \Delta P_{m,i}] \quad (14)$$

where the subindex “ $i$ ” is used to refer to each WEC in the wind park.

If all wind turbines have identical parameters and initial steady-state situations, the result is:  $\forall i = 1, 2, \dots, n$ ,  $A_{i,i} = A$ ,  $B_{i,i} = B$  and  $b_i = b$ , where  $A$ ,  $B$  and  $b$  are, respectively, the matrices and vector defined for one wind turbine, in the same way as (12) and (13). Consequently, for a wind park identified by the subindex  $\alpha$ , an equivalent linear dynamic system, shown in Fig. 3, can be defined as

$$\frac{dx_{\alpha}}{dt} = Ax_{\alpha} + Bu_{\alpha} + b \frac{\Delta P_{m,\alpha}}{n} \quad (15)$$

where

$$\begin{aligned} x_{\alpha} &= [\Delta E'_{\alpha} \quad \Delta E_{\alpha}^m \quad \Delta s_{\alpha}]^t \\ &= \frac{1}{n} \left[ \sum_{k=1}^n \Delta E_k^r \quad \sum_{k=1}^n \Delta E_k^m \quad \sum_{k=1}^n \Delta s_k \right]^t \end{aligned}$$

$$\begin{aligned} \bullet \quad u_{\alpha} &= \left[ \frac{\Delta U_{\alpha}^r}{(1/n) \sum_{k=1}^n \Delta U_k^r} \quad \frac{\Delta U_{\alpha}^m}{\sum_{k=1}^n \Delta U_k^m} \right]^t \\ \bullet \quad \Delta P_{m,\alpha} &= \sum_{k=1}^n \Delta P_{m,k} \end{aligned} =$$

On the other hand, the relations between voltage vector  $u_{\alpha}$  and the network can be made from the nodal analysis of electrical circuits. So, from Fig. 2, the result is

$$\begin{aligned} Y_{i,i} \Delta U_i - Y_{i,th} \Delta V &= Y_{s,i} \Delta E'_i \\ - \sum_{k=1}^n Y_{k,th} \Delta U_k + Y_{th,th} \Delta V &= 0 \end{aligned} \quad (16)$$

where

- $Y_{i,i} = Y_{s,i} + j\omega C_i + Y_{i,th}$ ;
- $Y_{th,th} = \sum_{k=1}^n Y_{k,th} + 1/Z_{th}$ ;
- $Y_{s,i} = 1/(R_{s,i} + jX'_i)$ ;
- $Y_{i,th} = 1/(R_{i,th} + jX_{i,th})$ .

Taking into account the  $\Delta U_{\alpha}$  variable, (15), (16), and assuming  $\forall i = 1, 2, \dots, n$ :  $Y_{i,i} = Y$ ,  $Y_{i,th} = Y_{th}$  and  $Y_{s,i} = Y_s$ , the new equations are

$$\left( Y - \frac{nY_{th}^2}{Y_{th,th}} \right) \Delta U_{\alpha} = Y_s \Delta E'_{\alpha} \quad (17)$$

$$-nY_{th} \Delta U_{\alpha} + Y_{th,th} \Delta V = 0. \quad (18)$$

In rectangular coordinates (17)

$$u_{\alpha} = \begin{bmatrix} \Delta U_{\alpha}^r \\ \Delta U_{\alpha}^m \end{bmatrix} = \begin{bmatrix} R & -X \\ X & R \end{bmatrix} \begin{bmatrix} \Delta E'_{\alpha}^r \\ \Delta E'_{\alpha}^m \end{bmatrix} \quad (19)$$

where

$$R + jX = \frac{Y_s}{\left( Y - \frac{nY_{th}^2}{Y_{th,th}} \right)}.$$

Putting (19) into (15), the new system is

$$\frac{dx_{\alpha}}{dt} = A' x_{\alpha} + b \frac{\Delta P_{m,\alpha}}{n} \quad (20)$$

where

$$A' = \begin{bmatrix} -v + v'R - w'X & w - v'X - w'R & \omega_s E_0^m \\ -w + v'X + w'R & -v + v'R - w'X & -\omega_s E_0^r \\ \frac{(-e - gR - mX)}{h} & \frac{(-f + gX - mR)}{h} & 0 \end{bmatrix}.$$

Assuming that (20) can be expressed in the steady-state situation by Fourier transform as

$$\underline{x}_{\alpha} = \frac{D \Delta P_{m,\alpha}}{n} \quad (21)$$

where

- $D = [D_1 \quad D_2 \quad D_3]^t = (j\Omega_0 \mathbf{1} - A')^{-1} b$
- $\Omega$  is the Fourier imaginary variable, that takes the rotational speed value,  $\Omega_0$ , of the excitation variable, in this case  $\Delta P_m(t)$ ;
- $\mathbf{1}$  is the unitary matrix;
- $b$  is the real vector  $[0 \quad 0 \quad 1/h]^t$
- $\Delta P_{m,\alpha}$  is the Fourier Transform of wind power fluctuation  $\Delta P_{m,\alpha}$  defined in (10) and (15)

The temporary variable  $\Delta P_{m,\alpha}$ , assuming zero for the initial angle, is defined as

$$\Delta P_{m,\alpha} = \sum_{k=1}^n P_{s,k} \sin(\theta_k + \Omega_0 t) = |\Delta P_{m,\alpha}| \sin(\Omega_0 t) \quad (22)$$

where

$$|\Delta P_{m,\alpha}| = \sqrt{\left(\sum_{k=1}^n P_{s,k} \sin(\theta_k)\right)^2 + \left(\sum_{k=1}^n P_{s,k} \cos(\theta_k)\right)^2}$$

So, the complex variable  $\Delta \underline{P}_{m,\alpha}$  in (21), can be expressed as:

$$\Delta \underline{P}_{m,\alpha} = |\Delta P_{m,\alpha}|. \quad (23)$$

Using (21) the  $\Delta E'$ ,  $\Delta s$  and  $\Delta \theta$  variables can be defined by the expressions

$$\Delta E_\alpha^r = X_1^r \sin(\Omega_0 t) + X_1^m \cos(\Omega_0 t) \quad (24)$$

$$\Delta E_\alpha^m = X_2^r \sin(\Omega_0 t) + X_2^m \cos(\Omega_0 t) \quad (25)$$

$$\Delta s_\alpha = X_3^r \sin(\Omega_0 t) + X_3^m \cos(\Omega_0 t). \quad (26)$$

Putting (23) in (24) and (25)

$$\Delta E_\alpha^r = \frac{1}{n} |\Delta P_{m,\alpha}| (D_1^r \sin(\Omega_0 t) + D_1^m \cos(\Omega_0 t)) \quad (27)$$

$$\Delta E_\alpha^m = \frac{1}{n} |\Delta P_{m,\alpha}| (D_2^r \sin(\Omega_0 t) + D_2^m \cos(\Omega_0 t)). \quad (28)$$

And consequently, using (18), the real and imaginary components of the modulus of voltage in the common node are

$$\begin{aligned} \begin{bmatrix} \Delta V^r \\ \Delta V^m \end{bmatrix} &= n \begin{bmatrix} V_1 & -V_2 \\ V_2 & V_1 \end{bmatrix} \begin{bmatrix} \Delta E_\alpha^r \\ \Delta E_\alpha^m \end{bmatrix} \\ &= \begin{bmatrix} V_1 & -V_2 \\ V_2 & V_1 \end{bmatrix} \begin{bmatrix} D_1^r & D_1^m \\ D_2^r & D_2^m \end{bmatrix} \begin{bmatrix} \sin(\Omega_0 t) \\ \cos(\Omega_0 t) \end{bmatrix} |\Delta P_{m,\alpha}| \end{aligned} \quad (29)$$

where

$$V_1 + jV_2 = \frac{Y_{\text{th}}}{Y_{\text{thth}} \underline{Y} - \frac{nY_{\text{th}}^2}{Y_{\text{thth}}}}$$

From (29), the following is obtained

$$\Delta V^r = |\Delta P_{m,\alpha}| (W_{1,1} \sin(\Omega_0 t) + W_{1,2} \cos(\Omega_0 t)) \quad (30)$$

$$\Delta V^m = |\Delta P_{m,\alpha}| (W_{2,1} \sin(\Omega_0 t) + W_{2,2} \cos(\Omega_0 t)) \quad (31)$$

where the constants  $W_{1,1}$ ,  $W_{1,2}$ ,  $W_{2,1}$  and  $W_{2,2}$  are obtained from (29).

So, the instantaneous variable  $v(t)$  can be defined as

$$v(t) = [V_0^r + \Delta V^r] \sin(\omega_s t) + [V_0^m + \Delta V^m] \cos(\omega_s t). \quad (32)$$

And the incremental modulus of  $v(t)$ , with respect to the initial value  $V_0$ , is

$$\begin{aligned} \Delta V(t) &= V(t) - V_0 \\ &= \sqrt{(V_0^r + \Delta V^r)^2 + (V_0^m + \Delta V^m)^2} - V_0 \\ &\approx \frac{V_0^r}{V_0} \Delta V^r + \frac{V_0^m}{V_0} \Delta V^m \end{aligned} \quad (33)$$

and consequently

$$\Delta V(t) = |\Delta P_{m,\alpha}| [K \sin(\Omega_0 t) + K' \cos(\Omega_0 t)] \quad (34)$$

where

- $K = (V_0^r W_{1,1} + V_0^m W_{2,1})/V_0$ ;
- $K' = (V_0^r W_{1,2} + V_0^m W_{2,2})/V_0$ .

Taking into account (34), the maximum voltage modulus fluctuation,  $\Delta V_{\text{max}}$ , can be defined, with respect to the average value  $V_0$ , as

$$\Delta V_{\text{max}} = |\Delta P_{m,\alpha}| \sqrt{K^2 + K'^2}. \quad (35)$$

## V. PROBABILISTIC MODEL OF AN ASYNCHRONOUS WIND PARK

The probabilistic model of mechanical power fluctuations in a wind park is based on the following hypotheses:

- i) The mechanical power fluctuations are produced by turbine rotation, and they have higher frequencies (1–2 Hz) than other wind power fluctuations (0.001–0.1 Hz).
- ii) During the analysis of the mechanical power fluctuations (high frequency), the mean values of wind turbine variables are constant. This is equivalent to assuming operating point values for wind turbine variables for high frequency studies; and the operating point values can be changed in the low frequencies interval.
- iii) The initial mechanical angles  $\theta_k$ , in (22), have constant values in the interval of mechanical power fluctuations (high frequency), and they change significantly with wind power fluctuations (low frequencies). The possible synchronization, assumed by several authors [14]–[17] is not considered because it has a very large time constant (a thousand seconds).
- iv) The initial values of the variables  $\theta_k$  are assumed to have a Uniform distribution function between 0 to  $2 \cdot \pi$
- v) All wind turbines have similar parameters, connection lines to network and operating point values. However, the model can be applied to a set of wind turbines

If the variable  $\theta_k$  is assumed as a statistical variable from uniform distribution, the circular functions  $\sin \theta_k$  and  $\cos \theta_k$  have statistical distribution functions with zero mean and  $1/\sqrt{2}$  standard deviation (see Appendix III).

On the other hand, assuming similar values for all  $P_{s,k}$  and taking into account the central limit theorem, the terms  $\zeta_1 = \sum_{k=1}^n P_{s,k} \sin \theta_k$  and  $\zeta_2 = \sum_{k=1}^n P_{s,k} \cos \theta_k$  in (22) are statistically independent and have Normal distribution functions with zero mean and standard deviation  $\sigma$ ,  $N(0, \sigma)$  (see Appendix III), where  $\sigma$  is defined as

$$\sigma = \sqrt{\sum_{k=1}^n \sigma_k^2} = \frac{1}{\sqrt{2}} \sqrt{\sum_{k=1}^n P_{s,k}^2}. \quad (36)$$

From (22),  $\xi = \sqrt{\zeta_1^2 + \zeta_2^2}$ , where  $\xi$  is a statistical variable associated to  $|\Delta P_{m,\alpha}|$  values.

So the variable  $(\xi^2/\sigma^2)$  is a 2-degree freedom  $\chi^2$  distribution (see Appendix III), with expectation  $M(\xi^2/\sigma^2) = 2$  and standard deviation  $D(\xi^2/\sigma^2) = 2$  [18]. Applying the approximated equations for statistical distribution [19], the result is

$$M\left(\sqrt{\frac{\xi^2}{\sigma^2}}\right) \approx \sqrt{\frac{49}{32}} \quad D\left(\sqrt{\frac{\xi^2}{\sigma^2}}\right) \approx \sqrt{\frac{15}{32}}$$

and, consequently, the expectation and standard deviation for a probability of 0.64 are (see Appendix III)

$$M(\xi) = \sqrt{\frac{49}{32}}\sigma = \sqrt{\frac{49}{64} \sum_{k=1}^n P_{s,k}^2} \approx 0.9 \sqrt{\sum_{k=1}^n P_{s,k}^2} \quad (37)$$

$$D(\xi) = \sqrt{\frac{15}{32}}\sigma = \sqrt{\frac{15}{64} \sum_{k=1}^n P_{s,k}^2} \approx 0.45 \sqrt{\sum_{k=1}^n P_{s,k}^2} \quad (38)$$

The density and distribution functions of the variable  $\xi'$ , normalization of  $\xi$ , with identical values  $P_{s,k} = 1$ , are shown in Appendix IV. In this case, the expectation and standard deviation are

$$M(\xi) = 0.9\sqrt{n}P_s \quad (39)$$

$$D(\xi) = 0.45\sqrt{n}P_s. \quad (40)$$

In conclusion, the aggregate dynamic system of an asynchronous wind park, with similar wind turbines, connection lines, and mean steady-state situations, can be modeled by an equivalent system, shown in Fig. 3. The mechanical power fluctuations of the aggregate system, taking into account (22), is defined probabilistically as

$$\Delta P_{m,\alpha}(t) = \xi \sin(\Omega_0 t) \quad (41)$$

where  $\xi$  is a statistical variable (see figures in Appendix III) of mean  $0.9\sqrt{n}P_s$  and standard deviation  $0.45\sqrt{n}P_s$ ,  $n$  is the number of wind turbines and  $P_s$  is the mechanical power fluctuations in one wind turbine.

From (27) and (28), assuming small changes in initial variable values of wind turbines, the probabilistic model of a wind park can be defined by the complex equivalent voltage source  $\underline{E}'_\alpha$ , such as

$$\Delta E_\alpha^r = \psi(\sin(\Omega_0 t + \varphi^r)) \quad (42)$$

$$\Delta E_\alpha^m = \psi(\sin(\Omega_0 t + \varphi^m)) \quad (43)$$

where

- $\varphi^r$  and  $\varphi^m$  are electrical angles obtained by single trigonometric transforms of (27) and (28).
- $\psi$  is a statistical variable of mean  $0.9P_s/\sqrt{n}$  and standard deviation  $0.45P_s/\sqrt{n}$ ,  $n$  is the number of wind turbines and  $P_s$  is the mechanical power fluctuations in one wind turbine.

Similarly, the probabilistic expression for the electrical variables of the wind park or network can be obtained ( $\Delta V$ ,  $\Delta I_s$ ,  $\Delta P_e$ , ...). The maximum voltage modulus fluctuation  $\Delta V_{\max}$  expressed in (35) is of highly practical interest, with the expectation expressed as

$$M(\Delta V_{\max,n}) = 0.9\sqrt{n}\Delta V_{\max,1} \quad (44)$$

where  $\Delta V_{\max,1} = P_s\sqrt{K^2 + K'^2}$  is the maximum voltage modulus fluctuation produced by one wind turbine.

A Monte Carlo simulation (5,000 experiments in a wind park with 100 turbines), with a nonaggregated model (see Appendix IV for equations and Appendix II for parameters), has been used to calculate the value of  $M(\Delta V_{\max})$ . A comparison with results obtained from the aggregated model using (44) is shown in Figs. 4 and 5.

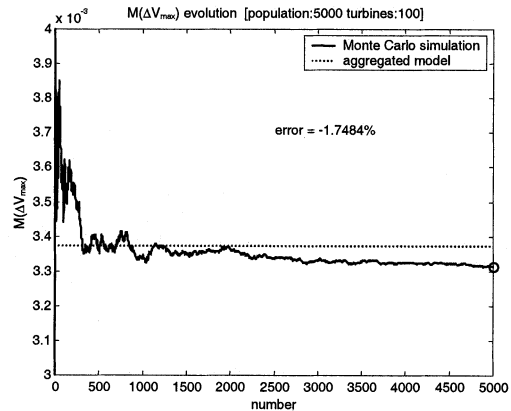


Fig. 4. Evolution of the mean value of  $\Delta V_{\max}$  during the Monte Carlo simulation.

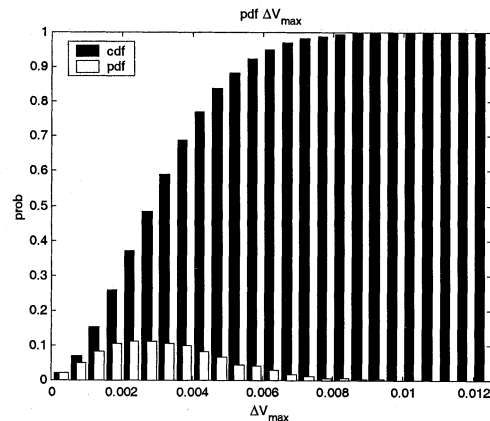


Fig. 5. Cumulative distribution function (cdf) and probability density function (pdf) of  $\Delta V_{\max}$  obtained with Monte Carlo simulation.

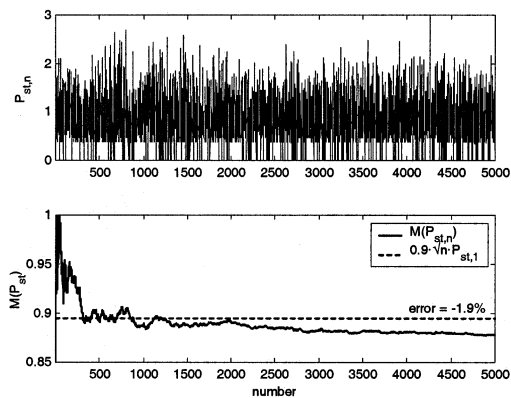


Fig. 6. Evolution of the mean value of  $P_{st,n}$  during the Monte Carlo simulation and the flickermeter depicted in IEC-868.

On the other hand, considering the properties of the flicker severity for short time,  $P_{st}$  [20], [24], the flicker produced by an asynchronous wind park with  $n$  similar machines  $P_{st,n}$  can be defined as (see Fig. 6)

$$M(P_{st,n}) = 0.9\sqrt{n}P_{st,1} \quad (45)$$

where  $P_{st,1}$  is the flicker produced by one wind turbine.

## VI. CONCLUSIONS

The aggregated model of a wind park obtained in this paper makes it possible to analyze and simulate mechanical power fluctuations, although the linear dynamic model can be used with other electrical or parametric perturbations.

From the aggregated system, a probabilistic model of wind parks was defined, where mechanical power fluctuations are present. The probabilistic model allows us to establish the probabilistic expression for mechanical power, voltage and current fluctuations. In addition, relations between voltage perturbations caused by a wind turbine and those caused by the wind park were established.

### APPENDIX I

#### NOTATION OF CONSTANTS AND VARIABLES

$\underline{E}$	complex number;
$E$ or $ E $	modulus of $\underline{E}$ ;
$E^r$	real part of $\underline{E}$ ;
$E^m$	imaginary part of $\underline{E}$ ;
$\mathbf{A}, \mathbf{a}$	matrix or vector;
$A, a$	constant or parameter;
$A_{i,j}, a_i$	elements of matrix $\mathbf{A}$ or vector $\mathbf{a}$ .

### APPENDIX II

#### MODEL DATA

##### Asynchronous Machine

$X_r$	rotor reactance 0.187 81 p.u.;
$X_s$	is the stator reactance 0.0639 p.u.;
$R_r$	rotor resistance 0.006 12 p.u.;
$R_s$	stator resistance 0.005 71 p.u.;
$X_m$	magnetization reactance 2.78 p.u.;
$H$	inertia 3.025s;
$\omega_s$	synchronous frequency $100\pi$ rad/s;
$p$	number of poles 4

$$T_0' = \frac{X_r + X_m}{\omega_s R_r}; X_0 = X_s + X_m; X' = X_s + \frac{X_r X_m}{X_r + X_m}$$

$I_s$	stator current;
$I_r$	rotor current;
$U$	output voltage.

##### Wind Turbine Parameters

$$r = 44.38;$$

$$P_s = 0.5 \text{ p.u..}$$

##### Network Parameters

$V_{th}$	1 p.u.;
$\underline{Y}_{th}$	admittance between network and wind turbine $-20 \cdot j$ p.u.;
$\underline{Y}_c$	capacitor admittance $0.29 \cdot j$ p.u.;
$\underline{Z}_{th}$	short circuit network impedance $5 \cdot 10^{-4} + 5 \cdot 10^{-3} \cdot j$ p.u..

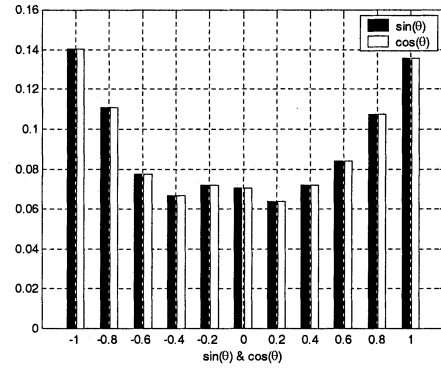


Fig. 7. Pdf of  $\cos \theta$  and  $\sin \theta$ .

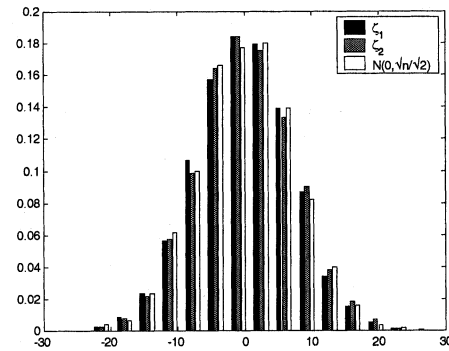


Fig. 8. Comparison between the pdf of  $\zeta_1, \zeta_2$  and the normal distribution  $N(0, \sqrt{n}/\sqrt{2})$ .

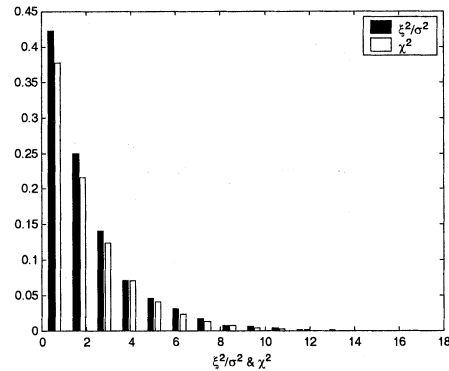


Fig. 9. Comparison between the pdf of  $\xi^2/\sigma^2$  and the distribution  $\chi^2$ .

### APPENDIX III

#### PROBABILITY DENSITY FUNCTION OF STATISTICAL VARIABLES

In Figures 7–10 and in Table I, the results of Monte Carlo simulation, with 5000 experiments and 100 wind turbines, are shown.

### APPENDIX IV

#### NONAGGREGATED MODEL EQUATIONS

In this Appendix IV, a comparison between the nonaggregated model and the aggregated model is shown.

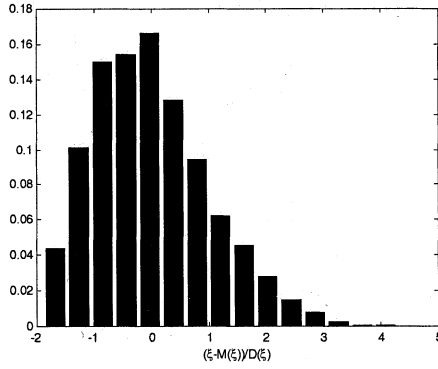
Fig. 10. Pdf of  $\xi' = (\xi - M(\xi))/D(\xi)$ .

TABLE I  
COMPARISON BETWEEN AGGREGATED MODEL  
AND MONTE CARLO SIMULATION

Variable	Monte Carlo		Aggr. Model	
	mean	$\sigma$	mean	$\sigma$
$\sin \theta$	-0.003	0.698	0	0.707
$\cos \theta$	0.015	0.716	0	0.707
$\zeta_1$	-0.002	7.073	0	7.071
$\zeta_1$	0.151	7.197	0	7.071
$\xi^2/\sigma^2$	2.029	2.031	2	2
$\xi$	8.905	4.647	9	4.5

Equations for the nonaggregated model are obtained by applying the nodal analysis in the system shown in Fig. 2, so

$$[\mathbf{Y}_{\text{node}}] \begin{bmatrix} \Delta U_1 \\ \vdots \\ \Delta U_n \\ \Delta V \end{bmatrix} = \mathbf{Y}_s \begin{bmatrix} \Delta E_1 \\ \vdots \\ \Delta E_n \\ 0 \end{bmatrix} \quad (46)$$

where

$$[\mathbf{Y}_{\text{node}}] = \begin{bmatrix} \underline{\mathbf{Y}} & 0 & \cdots & 0 & -\underline{\mathbf{Y}}_{\text{th}} \\ 0 & \underline{\mathbf{Y}} & \cdots & 0 & -\underline{\mathbf{Y}}_{\text{th}} \\ \vdots & \vdots & \ddots & \vdots & \vdots \\ 0 & 0 & \cdots & \underline{\mathbf{Y}} & -\underline{\mathbf{Y}}_{\text{th}} \\ -\underline{\mathbf{Y}}_{\text{th}} & -\underline{\mathbf{Y}}_{\text{th}} & \cdots & -\underline{\mathbf{Y}}_{\text{th}} & \underline{\mathbf{Y}}_{\text{th}} \end{bmatrix}_{(n+1) \times (n+1)}$$

The equation above can be written as

$$\begin{bmatrix} \Delta U_1^r + j\Delta U_1^m \\ \vdots \\ \Delta U_n^r + j\Delta U_n^m \\ \Delta V^r + j\Delta V^m \end{bmatrix} = [\mathbf{Y}_{\text{node}}]^{-1} \mathbf{Y}_s \begin{bmatrix} \Delta E_1^r + j\Delta E_1^m \\ \vdots \\ \Delta E_n^r + j\Delta E_n^m \\ 0 \end{bmatrix} \quad (47)$$

Assuming that (47) can be expressed in the steady state situation by Fourier Transform as

$$\begin{aligned} \Delta \underline{\mathbf{U}}^r &= \mathbf{Y}^r \Delta \underline{\mathbf{E}}^r - \mathbf{Y}^m \Delta \underline{\mathbf{E}}^m \\ \Delta \underline{\mathbf{U}}^m &= \mathbf{Y}^m \Delta \underline{\mathbf{E}}^r + \mathbf{Y}^r \Delta \underline{\mathbf{E}}^m \end{aligned} \quad (48)$$

where

- $\mathbf{Y}^r = \text{real} \left\{ [\mathbf{Y}_{\text{node}}]^{-1} \mathbf{Y}_s \right\}$ ;
- $\mathbf{Y}^m = \text{imag} \left\{ [\mathbf{Y}_{\text{node}}]^{-1} \mathbf{Y}_s \right\}$ ;
- $\Delta \underline{\mathbf{U}}^r = [\Delta U_1^r \ \cdots \ \Delta U_n^r \ \Delta V^r]^t$ ;
- $\Delta \underline{\mathbf{U}}^m = [\Delta U_1^m \ \cdots \ \Delta U_n^m \ \Delta V^m]^t$ ;
- $\Delta \underline{\mathbf{E}}^r = [\Delta E_1^r \ \cdots \ \Delta E_n^r \ 0]^t$ ;
- $\Delta \underline{\mathbf{E}}^m = [\Delta E_1^m \ \cdots \ \Delta E_n^m \ 0]^t$ .

Using the equation for asynchronous machines (1), the following equation is obtained:

$$\begin{bmatrix} \Delta E_i^r \\ \Delta E_i^m \\ \Delta S_i \end{bmatrix} = [j\Omega_0 \mathbf{1} - \mathbf{A}]^{-1} \times \left( \mathbf{B} \times \begin{bmatrix} \Delta U_i^r \\ \Delta U_i^m \end{bmatrix} + \mathbf{b} \times \Delta P_{m,i} \right) \quad (49)$$

And from (49)

$$\begin{bmatrix} \Delta E_i^r \\ \Delta E_i^m \end{bmatrix} = \begin{bmatrix} \underline{M}_{11} & \underline{M}_{12} \\ \underline{M}_{21} & \underline{M}_{22} \end{bmatrix} \begin{bmatrix} \Delta U_i^r \\ \Delta U_i^m \end{bmatrix} + \begin{bmatrix} \underline{N}_1 \\ \underline{N}_2 \end{bmatrix} \Delta P_{m,i} \quad (50)$$

where

- $[j\Omega_0 \mathbf{1} - \mathbf{A}]^{-1} \times \mathbf{B} = \begin{bmatrix} \underline{M}_{11} & \underline{M}_{12} \\ \underline{M}_{21} & \underline{M}_{22} \\ \underline{M}_{31} & \underline{M}_{32} \end{bmatrix}$ ;
- $[j\Omega_0 \mathbf{1} - \mathbf{A}]^{-1} \times \mathbf{b} = [\underline{N}_1 \ \underline{N}_2 \ \underline{N}_3]^t$ .

Using (50) and (48)

$$\begin{aligned} \Delta \underline{\mathbf{E}}^r &= \underline{M}_{11} \mathbf{1}_0 \Delta \underline{\mathbf{U}}^r + \underline{M}_{12} \mathbf{1}_0 \Delta \underline{\mathbf{U}}^m + \underline{N}_1 \Delta \underline{\mathbf{P}} \\ \Delta \underline{\mathbf{E}}^m &= \underline{M}_{21} \mathbf{1}_0 \Delta \underline{\mathbf{U}}^r + \underline{M}_{22} \mathbf{1}_0 \Delta \underline{\mathbf{U}}^m + \underline{N}_2 \Delta \underline{\mathbf{P}} \end{aligned} \quad (51)$$

where

- $\mathbf{1}_0 = \begin{bmatrix} 1 & 0 & \cdots & 0 \\ 0 & \ddots & & \vdots \\ \vdots & & 1 & \vdots \\ 0 & \cdots & \cdots & 0 \end{bmatrix}_{(n+1) \times (n+1)}$ ;
- $\Delta \underline{\mathbf{P}} = [\Delta P_{m,1} \ \cdots \ \Delta P_{m,n} \ 0]^t$ .

Then, nodal voltages can be obtained from

$$\begin{bmatrix} \Delta U^r \\ \Delta U^m \end{bmatrix} = \left( \mathbf{1} - \begin{bmatrix} \underline{\mathbf{Q}}_{11} & \underline{\mathbf{Q}}_{12} \\ \underline{\mathbf{Q}}_{21} & \underline{\mathbf{Q}}_{22} \end{bmatrix} \right)^{-1} \begin{bmatrix} \underline{\mathbf{S}}_1 \\ \underline{\mathbf{S}}_2 \end{bmatrix} \quad (52)$$

where

- $\underline{\mathbf{Q}}_{11} = (\underline{M}_{11} \mathbf{Y}^r - \underline{M}_{21} \mathbf{Y}^m) \mathbf{1}_0$ ;
- $\underline{\mathbf{Q}}_{12} = (\underline{M}_{12} \mathbf{Y}^r - \underline{M}_{22} \mathbf{Y}^m) \mathbf{1}_0$ ;
- $\underline{\mathbf{Q}}_{21} = (\underline{M}_{11} \mathbf{Y}^m + \underline{M}_{21} \mathbf{Y}^r) \mathbf{1}_0$ ;
- $\underline{\mathbf{Q}}_{22} = (\underline{M}_{12} \mathbf{Y}^m + \underline{M}_{22} \mathbf{Y}^r) \mathbf{1}_0$ ;
- $\underline{\mathbf{S}}_1 = (\underline{N}_1 \mathbf{Y}^r - \underline{N}_2 \mathbf{Y}^m) \Delta \underline{\mathbf{P}}$ ;
- $\underline{\mathbf{S}}_2 = (\underline{N}_1 \mathbf{Y}^m + \underline{N}_2 \mathbf{Y}^r) \Delta \underline{\mathbf{P}}$ ;

The network voltage components are the  $n + 1$  elements of  $\Delta \underline{\mathbf{U}}_r$  and  $\Delta \underline{\mathbf{U}}_m$  vectors:

$$\begin{aligned} \Delta \underline{V}^r &= \Delta V_1^r + j\Delta V_2^r = \Delta \underline{\mathbf{U}}^r [n + 1] \\ \Delta \underline{V}^m &= \Delta V_1^m + j\Delta V_2^m = \Delta \underline{\mathbf{U}}^m [n + 1]. \end{aligned} \quad (53)$$

The maximum voltage modulus fluctuation,  $\Delta V_{\text{max}}$ , can be defined, with respect to the average value  $V_0$ , as

$$\Delta V_{\text{max}} = \frac{\sqrt{K_1^2 + K_2^2}}{V_0} \quad (54)$$

where

- $K_1 = (V_0^r \Delta V_1^r + V_0^m \Delta V_2^r) / V_0$
- $K_2 = (V_0^r \Delta V_1^m + V_0^m \Delta V_2^m) / V_0$

#### REFERENCES

- [1] A. Feijóo, J. Cidrás, and J. L. G. Dornelas, "Wind speed simulation in wind farms for steady-state security assessment of electrical power systems," *IEEE Trans. Energy Conversion*, vol. 14, pp. 1582–1588, Feb. 2000.
- [2] P. Gardner, "Flicker from wind farms," in *Proc. BWEA/RAL Workshop on Wind Energy into Weak Electricity Networks*, June 1993, pp. 27–37.
- [3] A. Larson, "Flicker and slow voltage variations from wind turbines," in *Proc. 7th ICHQP*, Las Vegas, 1996.
- [4] N. G. Mortensen, L. Landberg, and I. Troen, *Wind Atlas Analysis and Application Program (WASP)*, 1993.
- [5] L. L. Freris, *Wind Energy Conversion Systems*: Prentice-Hall, 1990.
- [6] P. M. Anderson and S. Bose, "Stability of wind turbine systems," *IEEE Trans. Power Appar. Syst.*, vol. PAS-102, no. 12, Dec. 1983.
- [7] A. E. Feijóo, "Influencia de los Parques Eólicos en la Seguridad Estacionaria y Calidad de Onda de Redes Eléctricas de Gran Dimensión," Ph.D. (in Spanish), Universidade de Vigo, Spain, 1998.
- [8] G. J. Rogers, J. D. Manno, and R. T. H. Alden, "An aggregate motor model for industrial plants," *IEEE Trans. Power Appar. Syst.*, vol. PAS-103, no. 4, Apr. 1984.
- [9] F. Nozari, M. D. Kankam, and W. W. Price, "Aggregatoion of inductions motors for transient stability load modeling," *IEEE Trans. Power Syst.*, vol. PWRS-2, Nov. 1987.
- [10] A. M. Stankovic and B. C. Lesieutre, "A probabilistic approach to aggregate induction machine modeling," *IEEE Trans. Power Syst.*, vol. 11, Nov. 1996.
- [11] P. Pillay, S. M. A. Sabur, and M. M. Haq, "A model for induction motor aggregation for power system studies," *Elect. Power Syst. Res.*, no. 42, 1997.
- [12] T. Y. J. Lem and R. T. H. Alden, "Comparison of experimental and aggregate induction motor responses," *IEEE Trans. Power Syst.*, vol. 9, pp. 1985–1990, Nov. 1994.
- [13] D. S. Brereton, D. G. Lewis, and C. C. Young, "Representation of induction motor loads during power system stability studies," *AIEE Trans.*, vol. 76, pp. 451–461, Aug. 1957.
- [14] R. Klosee, F. Santjer, and G. Gerdes, "Flickerbewertung bei windenergieanlagen" (in German), *DEWI Magazine*, no. 11, Aug. 1997.
- [15] J. O. G. Tande, "Synchronization of wind turbines," in *Proc. Wind Power for the 21st Century*, Kassel, Germany, Sept. 25–27, 2000.
- [16] A. Stampa, "Synchronization von netzgekoppelten windenergieanlagen in einem windpark," *DEWI Magazine*, no. 7, Aug. 1995.
- [17] J. Cidrás, A. Feijoo, and C. Carrillo, "Synchronization of asynchronous wind turbines," *Abstract published in IEEE Power Eng. Rev.*, May 2002.
- [18] S. Ríos, *Métodos Estadísticos*: Ediciones del Castillo, 1977, pp. 222–223.
- [19] K. C. Kapur and L. R. Lamberson, *Reliability in Engineering Design*. New York: Wiley, 1977, pp. 101–102.
- [20] P. Sørensen, "Methods for Calculation of the Flicker Contributions from Wind Turbines," Risø National Laboratory, Risø-I-939 (EN), 1995.
- [21] S. M. Petersen, "Wind Turbine Test. Vestas V27–225 kW," Risø National Laboratory, Risø-M-2861, 1990.
- [22] T. Thiringer, "Power quality measurements performed on a low-voltage grid equipped with two turbines," *IEEE Trans. Energy Conversion*, vol. 8, pp. 520–526, Sept. 1993.
- [23] T. Thiringer and A. Dahlberg, "Periodic pulsations form a three-bladed wind turbine," *IEEE Trans. Energy Conversion*, vol. 16, no. 2, pp. 128–133, June 2001.
- [24] "Electromagnetic Compatibility (EMC)-Part 4: Testing and Measurement Techniques-Section 15: Flickermeter-Functional and Design Specifications," IEC 61 000–4-15, 1997.

**José Cidrás Pidre** (M'86) received the Ph.D. degree in electrical engineering from the Universidade de Santiago de Compostela, Spain, in 1987.

Currently, he is professor in the Departamento de Enxeñaría Eléctrica of the Universidade de Vigo, Spain, and leads some investigation projects in wind energy, photovoltaics, and planning of power systems.

**Camilo José Carrillo** received the Ph.D. degree in electrical engineering from the Universidade de Vigo (Spain) in 2001.

Currently, he is with the Departamento de Enxeñaría Eléctrica of the Universidade de Vigo and his current interest is wind energy.

**Andrés Elías Feijóo Lorenzo** received the Ph.D. degree in electrical engineering from the Universidade de Vigo, Spain, in 1998.

Currently, he is with the Departamento de Enxeñaría Eléctrica of the Universidade de Vigo and his current interest is wind energy and power quality.